Synthesis of Classical, Three-Carbon-Bridged 5-Substituted Furo[2,3-*d*]pyrimidine and 6-Substituted Pyrrolo[2,3-*d*]pyrimidine Analogues as Antifolates[1]

Aleem Gangjee,*,† Yibin Zeng,†,‡ John J. McGuire,§ Farideh Mehraein,§ and Roy L. Kisliuk||

Division of Medicinal Chemistry, Graduate School of Pharmaceutical Sciences, Duquesne University, Pittsburgh, Pennsylvania 15282, Grace Cancer Drug Center, Roswell Park Cancer Institute, Elm and Carlton Streets, Buffalo, New York 14263, and Department of Biochemistry, Tufts University School of Medicine, Boston, Massachusetts 02111

Received June 30, 2004

Bridge homologation of the previously reported classical two-carbon-bridged antifolates, a 5-substituted 2,4-diaminofuro[2,3-*d*]pyrimidine (**1**) [which is a 6-regioisomer of LY231514 (Alimta)] and a 6-subsituted 2-amino-4-oxopyrrolo[2,3-*d*]pyrimidine, afforded the three-carbon-bridged antifolates analogues **4** and **5**, with enhanced inhibitory activity against tumor cells in culture (EC_{50} values in the $10^{-8}-10^{-7}$ M range or less). These two analogues were synthesized via a 10-step synthetic sequence starting from methyl 4-bromobenzoate (**14**), which was elaborated to the α-chloromethyl ketone (**8**) followed by condensation with 2,6-diaminopyrimidin-4-one (**7**) to afford the substituted furo[2,3-*d*]pyrimidine **9** and the pyrrolo[2,3-*d*]-pyrimidine **10**. Subsequent coupling of each regioisomer with diethyl-L-glutamate followed by saponification afforded **4** and **5**. The biological results indicate that elongation of the C8−C9 bridge of the classical 5-substituted 2,4-diaminofuro[2,3-*d*]pyrimidine and 6-substituted 2-amino-4-oxopyrrolo[2,3-*d*]pyrimidine are highly conducive to antitumor activity in vitro, despite a lack of increase in inhibitory activity against the target enzymes. This supports our original hypothesis that truncation of the B-ring of a highly potent 6−6 ring system to a 6−5 ring system can be compensated by bridge homologation to restore the overall length of the molecule.

Introduction

Folate metabolism has long been recognized as an effective target for chemotherapy, due to its crucial role in the biosynthesis of nucleic acid precursors.[2] Inhibitors of folate-dependent enzymes have found clinical utility as antitumor, antimicrobial, and antiprotozoal agents.[3,4]

As part of a continuing effort to develop novel classical antifolates as DHFR inhibitors and as antitumor agents, Gangjee et al.[5] reported the synthesis of *N*-[4-[2-(2,4-diaminofuro[2,3-*d*]pyrimidin-5-yl)ethyl]benzoyl]-L-glutamic acid (**1**) as a novel 6−5 bicyclic antifolate. Despite its reasonably potent inhibitory activity against the growth of tumor cells in culture (EC_{50}·$10^{-7}-10^{-8}$ M), its dihydrofolate reductase (DHFR) inhibitory potency was low ($IC_{50} = 10^{-6}$ M) compared to 2,4-diamino 6−6 bicyclic analogues such as methotrexate (MTX) ($IC_{50} = 22 \times 10^{-9}$ M). We have recently demonstrated that a simple alkylation of the C9 position of the C8−C9 bridge region of **1** enhances the inhibition of DHFR such as in compounds **2** and **3**.[6,7] Compared to **1**, the C9-methyl analogue **2** ($IC_{50} = 0.42 \times 10^{-6}$ M) was twice as inhibitory against recombinant human (rh) DHFR, while the C9-ethyl analogue **3** ($IC_{50} = 0.22 \times 10^{-6}$ M) was twice as potent as analogue **2**.[6,7] Both **2** and **3** were about 10-fold greater in their growth inhibitory potency against tumor cells in culture with EC_{50} values in the nanomolar range as compared to **1**.[6,7] The increased potency against DHFR as well as against the growth of tumor cells in culture of **2** and **3** were, in part, attributed to increased hydrophobic interaction of the C9-alkyl moiety with DHFR and by their increased lipophilicity. In this report we describe an alternate approach to improve the antitumor activity of **1** via bridge homologation.

A possible reason for the low DHFR inhibitory activity of **1** and its relatively low activity against tumor cell growth in culture compared to MTX could be that truncation of the 6−6 bicyclic system (of MTX-like compounds) to a 6−5 ring system shortens the overall length of the molecule, which results in less than optimal enzyme interaction and antitumor activity. Molecular modeling studies using SYBYL 6.6 [8] and its energy minimization options suggested that the distance and orientation of the α-carboxyl group of the glutamate of **1** with respect to the pyrimidine ring fell short by approximately one carbon, compared to that of the bound conformation of MTX in rhDHFR. The α-carboxylate group has important charge-mediated interactions with DHFR.[9] Thus, homologation of the two-carbon bridge of **1** to a three-carbon bridge might restore the appropriate position for the α-carboxyl group and thus increase the potency against DHFR and perhaps improve the antitumor activity against tumor cells in culture as well. Support for this idea comes from TNP-351,[10] a three-carbon-bridged pyrrolo[2,3-*d*]pyrimidine analogue of **1** that is a highly potent DHFR inhibitor

* To whom correspondence should be addressed. Tel: (412) 396−6070. Fax: (412) 396−5593. E-mail: gangjee@duq.edu.
† Duquesne University.
‡ Current address: Department of Medicinal Chemistry, The University of Kansas, Lawrence, KS 66045.
§ Roswell Park Cancer Institute.
|| Tufts University School of Medicine.

10.1021/jm040123k CCC: $27.50
Published on Web 12/08/2004

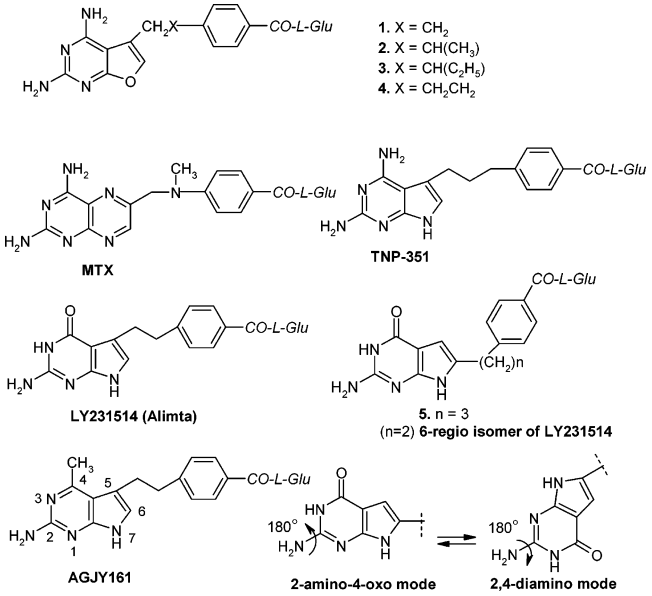

Figure 1.

and which is currently in clinical trials in Japan as an antitumor agent. Thus, compound **4**, the three-carbon-bridged analogue of **1** and a furo isostere of TNP-351, was designed and synthesized to explore its antitumor activity.

Gangjee et al.[11] recently reported that in 6−5 ring-fused pyrrolo[2,3-*d*]pyrimidine systems such as the 4-methyl analogue of LY231514, AGJY161 (Figure 1), the 7-NH mimics the 4-amino group of MTX by rotation of 180° around the C_2-NH_2 bond when bound to DHFR. LY231514 is reported to be a dual TS-DHFR inhibitor (hTS K_i = 340 nM; hDHFR K_i = 7 nM).[12] Since the 2-amino-4-oxo portion of the pyrimidine ring is the preferred binding mode for classical antifolates to TS [e.g. 2-amino-4-oxo-*N*10-propargyl-5,8-dideazafolate (PDDF)],[13] and the 2,4-diamino portion of the pyrimidine ring is the preferred binding mode for DHFR (e.g. MTX),[9] a possible reason for the dual TS and DHFR inhibitory activity of LY131514 could be the ability of the 2-amino-4-oxopyrrolo[2,3-*d*]pyrimidine to adopt both the "2-amino-4-oxo" mode as well as "2,4-diamino" mode (Figure 1) via rotation of the C_2-NH_2 bond by 180°, using the pyrrole NH to mimic the 4-amino group of MTX.

The 6-regioisomer of LY231514 (Figure 1) was previously synthesized by Taylor et al.[14] and was reported to be inactive in cell culture. The first step in the synthetic sequence for **4** (Scheme 2) also afforded the precursor to the 6-substituted three-carbon-bridged pyrrolo[2,3-*d*]pyrimidine **5**. Thus it was of interest to synthesize compound **5** as a homologue of the 6-regioisomer of LY231514 (Figure 1) with increased conformational flexibility in the side chain.

Polyglutamylation via folylpolyglutamate synthetase (FPGS) is an important mechanism for trapping classical folates and antifolates within the cell, thus maintaining high intracellular concentrations and in some instances for increasing binding affinity for folate-dependent enzymes and antitumor activity.[6,11] Thus, it was also of interest to determine the effect of homologation of the bridge length of the classical, two-carbon-bridged, 5-substituted 2,4-diaminofuro[2,3-*d*]pyrimidine and 6-substituted 2-amino-4-oxopyrrolo[2,3-*d*]pyrimidine to three carbons with respect to FPGS activity.

Chemistry

It was anticipated that a Wittig condensation of 5-chloromethyl-2,4-diaminofuro[2,3-*d*]pyrimidine (**6**) with a suitably substituted phenyl acetylaldehyde followed by catalytic reduction would afford the skeleton of target compound **4** (route A, Figure 2). However, in a model reaction using phenylacetaldehyde, the olefinic intermediate was isolated in 35% yield as an *E*/*Z* mixture. Reduction of the double bond afforded the desired product in only 20% isolated yield. Furthermore, synthesis of the commercially unavailable, substituted phenylacetaldehyde afforded low yields.

An alternate route was devised from the retrosynthetic analysis of the target skeletons (**9** and **10**) (route B, Figure 3), where a single step cyclocondensation of 2,6-diaminopyrimidin-4-one **7** with a suitable α-halo ketone **8**[15] would afford both the furo[2,3-*d*]pyrimidine and the pyrrolo[2,3-*d*]pyrimidine.

In our recent investigations[16] of the cyclocondensation of **7** with various α-chloro ketones, we found that both **12** and **13** could be obtained as a mixture of regioisomers in a single reaction by careful monitoring of the reaction conditions. Separation of the isomers afforded pure **12** and **13** in good yield (50−70%). The desired α-chloromethyl ketone **8** could, in turn, be obtained from commercially available substituted bromobenzene and 3-butyn-1-ol.

Thus, palladium-catalyzed coupling of methyl 4-bromobenzoate (**14**) with 3-butyn-1-ol (**15**)[17] (Scheme 1) afforded phenylbutynyl alcohol **16** (75%), which was catalytically hydrogenated to give the saturated alcohol **17** in quantitative yield. Subsequent oxidation of **17** using Jones' reagent[18] afforded the carboxylic acid **18** (65%), which was converted to the acid chloride **19** and immediately reacted with diazomethane followed by

Scheme 1

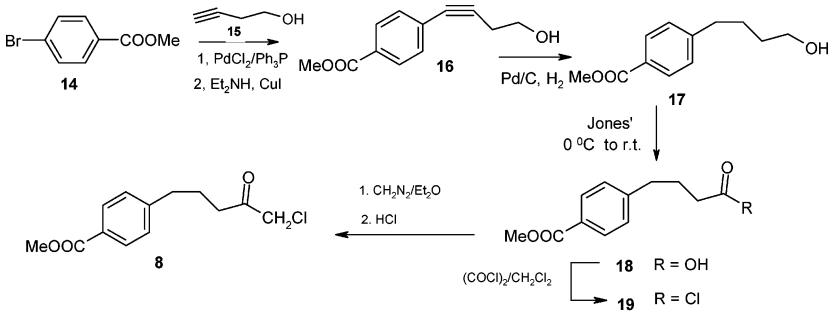

Scheme 2

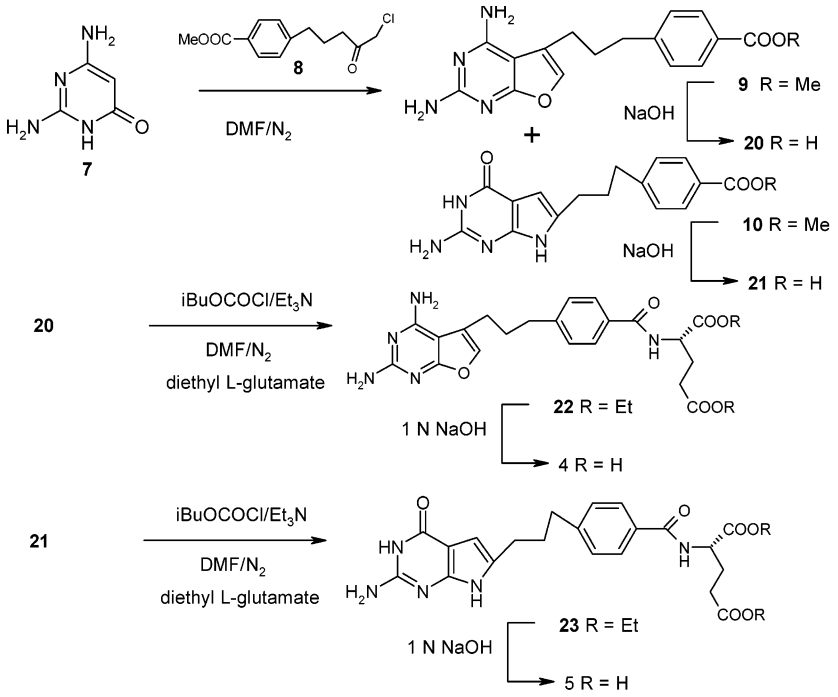

concentrated HCl to give the desired α-chloro ketone **8** in 75% yield over three steps.[19]

With the desired α-chloro ketone **8** at hand, the next step was the condensation of 2,6-diaminopyrimidin-4-one **7** with **8** (Scheme 2). Using DMF as the solvent at room temperature for 24 h, compound **9** was obtained in 10% yield along with the recovery of starting materials. Increasing the reaction temperature and time afforded both **9** and **10**. Optimal yields were obtained at 40−45 °C for 3 days and **9** and **10** were each isolated, after chromatographic separation, in 40% yield (80% total).

Hydrolysis of **9** and **10** afforded the corresponding free acids **20** and **21** (90−92%). Subsequent coupling with L-glutamate diethyl ester using isobutyl chloroformate

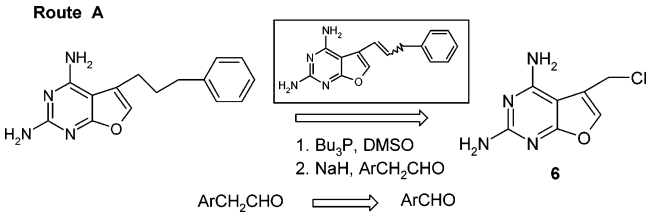

Figure 2.

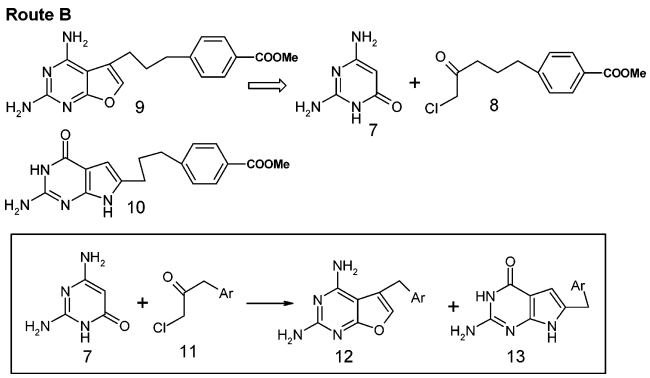

Figure 3.

Table 1. Inhibitory Concentration (IC_{50} in μM) against Isolated DHFR and TS[a]

	DHFR			TS		
	rh[c]	ec[d]	lc	rh[e]	ec[e]	lc
1[b]	1.0	ND[b]	0.1	220	ND	200
4	9.0	7.0	11	>18	>180	>100
5	>21 (16%)	22	>110	>17	>180	>100
MTX	0.022	0.007	0.022	ND	ND	ND
PDDF[f]	ND	ND	ND	0.18	0.09	0.009
LY231514[g]	2.3	230	230	19	38	38

[a] The percent inhibition was determined at a minimum of four inhibitor concentrations with 20% of the 50% point. The standard deviations for determination of IC_{50} values were within ±10% of the value given. [b] Data derived from ref 5; ND = not determined. [c] rhDHFR kindly provided by J. H. Freisheim, Medical College of Ohio, Toledo, OH. [d] *E. coli* DHFR kindly provided by Dr. R. L. Blakley, St. Jude's Children's Research Hospital, Memphis, TN. [e] rh TS and *E. coli* TS kindly provided by Dr. Frank Maley, New York State Department of Health, Albany, NY. [f] PDDF kindly provided by Dr. M. G. Nair, University of South Alabama, Mobile, AL. [g] LY231514 (Alimta) kindly provided by Dr. Chuan Shih, Eli Lilly and Co., Indianapolis, IN.

as the activating agent[17] afforded the diesters **22** and **23**. Final saponification of the diesters gave the desired diacids **4** and **5** respectively.

Biological Evaluation and Discussion

DHFR and TS Inhibition. Compounds **4** and **5** were evaluated as inhibitors of *Escherichia coli* (ec), *Lactobacillus casei* (lc), and recombinant human (rh) DHFR.[17] The inhibitory potency (IC_{50}) values are listed in Table 1 and compared with MTX as well as the previously reported values for **1**.[5] For rhDHFR, the 5-substituted, three-carbon-bridged furo[2,3-*d*]pyrimidine analogue **4** was about 400-fold less potent than MTX, 4-fold less potent than LY231514, and 9-fold less potent than the two-carbon-bridged analogue **1**. The 6-substituted, three-carbon-bridged analogue **5** was poorly active with an IC_{50} > 21 μM.

Table 2. Activity of **4** and **5** as Substrates for Recombinant Human FPGS[a]

substrate	K_m, μM	$V_{max,rel}$	V_{max}/K_m	n
aminopterin	4.5 ± 1.4	1.00	0.22	7
1[b]	8.5 ± 2.1	0.65 ± 0.01	0.07	3
4	0.3 ± 0	0.42 ± 0.02	1.4	2
5	0.9 ± 0.1	0.57 ± 0.06	0.63	2

[a] FPGS substrate activity was determined as described in the ref 6 at 2 mM L-[^{3}H]glutamate. Values presented are average ± SD if $n \geq 3$ and average ± range for $n = 2$. V_{max} values are calculated relative to aminopterin within the same experiment. [b] Data from ref 5.

Against ecDHFR, compound **4** had similar potency as against rhDHFR and compound **5** was 3-fold less potent. Compound **4** also inhibited lcDHFR at a level similar to its inhibition of rhDHFR and compound **5** was essentially inactive, while the parent two-carbon-bridged analogue **1** had a 10-fold increase in potency compared to its rhDHFR inhibition.

Analogues **4** and **5** were also evaluated as inhibitors of ecTS, lcTS, and rhTS[6,7] and compared to PDDF as a control. Both analogues were inactive at the concentrations tested (Table 1).

FPGS Substrate Activity. Since polyglutamylation by the enzyme FPGS can significantly enhance the antitumor activity of some classical antifolates, such as LY231514 and TNP-351,[14,20] it was of interest to evaluate these analogues as substrates of FPGS. Their activity was evaluated in vitro with recombinant human FPGS and compared to that of AMT, a good substrate for FPGS. The data (Table 2) show that both **4** and **5** are very efficient substrates for human FPGS, despite their 2-fold lower V_{max} values, because of substantial decreases in K_m. Compound **4** was 6-fold more efficient than AMT, while **5** was 3-fold more efficient than AMT. These results suggest that metabolism to polyglutamates must be considered in the mechanism of action of both **4** and **5**. It is interesting to note that modification of the bridge region of the classical 2,4-diaminofuropyrimidine **1** has significant effects on FPGS substrate activity. Compared to the two-carbon-bridged compound **1**, the three-carbon-bridged compound **4** is 20-fold more efficient as a FPGS substrate.

In Vitro Human Tumor Cell Growth Inhibition. The growth inhibitory potency of **4** and **5** were compared to that of MTX in continuous exposure against the CCRF-CEM human lymphoblastic leukemia[21] and a series of MTX-resistant sublines[22−24] (Table 3). The three-carbon-bridged 2,4-diaminofuro[2,3-*d*]pyrimidine analogue **4** was highly cytotoxic against the growth of CCRF-CEM cells in culture with an EC_{50} of 60 nM, which was about 5-fold more potent than its parent compound **1**. Interestingly, compound **5**, the three-carbon-bridged 2-amino-4-oxopyrrolo[2,3-*d*]pyrimidine analogue, also had reasonable inhibitory potency against the growth of CCRF-CEM cells in culture with an EC_{50} of 460 nM, which was unexpected since the 6-regioisomer of LY231514 was reported to be inactive in culture with an $EC_{50} > 60$ μM.[11] This indicates that elongation of the bridge length from two carbons to three carbons for the classical 5-substituted 2,4-diaminofuro[2,3-*d*]-pyrimindine and the 6-substituted 2-amino-4-oxo-pyrrolo[2,3-*d*]pyrimidine is highly conducive to tumor growth inhibition in culture and could be the result of the polyglutamate metabolites of **4** and **5**.

Table 3. Growth Inhibition of Parental CCRF-CEM Human Leukemia Cells and Sublines with Single, Defined Mechanisms of MTX Resistance during Continuous (0−120 h) Exposure to MTX, **4**, or **5**[a]

	EC_{50}, nM			
drug	CCRF-CEM	R1[b] (↑ DHFR)	R2[c] (↓ uptake)	R30dm[d] (↓ Glu_n)
MTX	8.2 ± 0.2	660 ± 50	1500 ± 0	7.9 ± 0.4
1[e]	290 ± 10	nd[f]	nd[f]	4250 ± 50
4	60 ± 14	≥4600	1050 ± 50	84 ± 8
5	460 ± 10	860 ± 150	4350 ± 650	470 ± 60

[a] All values presented are average ± range for $n = 2$. [b] CCRF-CEM subline resistant to MTX solely as a result of a 20-fold increase in wild-type DHFR protein and activity.[20] [c] CCRF-CEM subline resistant as a result of decreased uptake of MTX.[21] [d] CCRF-CEM subline resistant to MTX solely as a result of decreased polyglutamylation; this cell line has 1% of the FPGS specific activity (measured with MTX as the folate substrate) of parental CCRF-CEM.[22] [e] Data from ref 5. [f] nd = not determined.

DHFR overexpressing line R1 was >76-fold cross-resistant to **4**, similar to the resistance to MTX, indicating that DHFR is likely the primary target of this 2,4-diaminofuropyrimidine. In contrast, R1 was <2-fold cross-resistant to **5**, suggesting that it primarily inhibits a site other than DHFR. The MTX-transport-resistant subline R2, which does not express functional reduced folate carrier (RFC),[25] is 17-fold cross-resistant to **4** and 10-fold resistant to **5**, while it is 180-fold resistant to MTX. The data suggest that both **4** and **5** utilize the RFC as their primary means of transport, but at high extracellular levels, both drugs are able to diffuse through the plasma membrane. A cell line expressing low levels of folylpolyglutamate synthetase (FPGS) is not cross-resistant to either analogue under continuous exposure conditions. This means either that each monoglutamate is a potent inhibitor of its respective target (as is MTX), which is inconsistent with the enzyme inhibition data (Table 1), or that each analogue is efficiently polyglutamylated even at low FPGS levels, indicating that they are efficient substrates, which is consistent with their high efficiency as FPGS substrates (Table 2).

Metabolite protection studies were performed to further elucidate the mechanism of action of **4** and **5**. At concentrations of drug that inhibited the growth of CCRF-CEM cells by ≥90%, leucovorin was able to fully protect against the effects of MTX, **4**, and **5** (data not shown). This is consistent with an antifolate mechanism of action for **4** and **5**. Further studies in CCRF-CEM cells examined the ability of thymidine (TdR) and hypoxanthine (Hx) to protect against growth inhibition. These metabolites can be salvaged to produce dTTP and the purine NTPs required for DNA synthesis and thus bypass the MTX blockade.[26] As described in the methods, in T-lymphoblast cell lines such as CCRF-CEM, TdR can only be tested in the presence of dCyd, which reverses its toxic effects; however, dCyd has no protective effect on MTX either alone or in paired combination with either Hx or TdR (Table 4, footnote *a*). The data (Table 4) show that for **4**, neither TdR nor Hx alone protected to any significant extent; both metabolites were required to achieve significant protection. This indicates that both purine and thymidylate synthesis are inhibited, and this is consistent with DHFR being the primary target of **4**. In contrast, Hx alone could protect against growth inhibition by **5** and addition of

Table 4. Protection of CCRF-CEM Human Leukemia Cells against the Growth Inhibitory Effects of MTX, **4**, and **5** by 10 μM Hypoxanthine (Hx), 5 μM Thymidine (TdR), and Their Combination

	relative growth (%)[a,b]			
drug	no addition	5 μM TdR	10 μM Hx	Hx + TdR
MTX (30 nM)	13 ± 0	16 ± 0	15.5 ± 0.5	74.5 ± 6.5
4	21 ± 0	25.5 ± 0.5	20 ± 0	73.5 ± 2.5
MTX	11 ± 0	12.5 ± 0.5	13.5 ± 0.5	73.5 ± 0.5
5	12 ± 0	11 ± 0	80.5 ± 0.5	76 ± 1

[a] Deoxycytidine (dCyd; 10 μM) was present in all the above cultures to prevent the inhibition of growth caused in T-cell leukemias such as CCRF-CEM by TdR (see the methods). In typical results, dCyd alone had no effect on CCRF-CEM growth (97 ± 3% of control) and did not protect against growth inhibition by any of these drugs (data not shown). Hx alone (98 ± 1% of control) or in the presence of dCyd (94 ± 0% of control) did not affect CCRF-CEM growth and did not protect against MTX-induced growth inhibition (Table above). TdR alone inhibited growth of CCRF-CEM (35 ± 0% of control), but TdR+dCyd was essentially not growth inhibitory (95 ± 2% of control) and neither protected against MTX-induced growth inhibition (table above). Similarly, Hx + TdR + dCyd did not appreciably inhibit growth of CCRF-CEM (95.5 ± 2.5% of control). [b] Growth is expressed relative to quadruplicate cultures not treated with either drug or metabolite and is the average ± range for duplicate treated samples. Each experiment was repeated for each drug with similar results.

other metabolites did not improve the protection. These data suggest that **5** inhibits purine synthesis only; this is also consistent with the lack of cross-resistance of the DHFR overproducing R1 (Table 3). Since there are two folate-dependent formyltransferases in purine synthesis, it would be of interest to know which is inhibited. Current anti-purine antifolates are primarily targeted to GAR formyltransferase.[27]

Compounds **4** and **5** were selected by the National Cancer Institute[28] for evaluation in its in vitro preclinical antitumor screening program. The ability of compounds **4** and **5** to inhibit the growth of 54 tumor cell lines was measured as GI_{50} values, the concentration required to inhibit the growth of tumor cells in culture by 50% as compared to the control. In more than 10 cell lines, compound **4** showed GI_{50} values in the $10^{-9}-10^{-7}$ M range (Table 5) and compound **5** showed GI_{50} values in the $10^{-8}-10^{-7}$ M in eight cell lines. It was interesting to note that compounds **4** and **5** were not general cell poisons but showed selectivity both within a type of tumor cell line as well as across different tumor cell lines with inhibitory values that in some instances differed by 10 000-fold. Compound **4** is currently under further evaluation by the NCI as an antitumor agent.

In summary, classical, three-carbon-bridged, 5-substituted 2,4-diaminofuro[2,3-*d*]pyrimidine (**4**) and 6-substituted 2-amino-4-oxopyrrolo[2,3-*d*]pyrimidine (**5**) were designed and synthesized. The biological results indicate that elongation of the C8−C9 bridge of the classical, 5-substituted furo[2,3-*d*]pyrimidine to a three-carbon bridge (analogue **4**) increases (5-fold) the inhibitory activity against the growth of tumor cells in culture compared to the two-carbon-bridged parent, compound **1**. Homologation of the C8−C9 bridge of the classical, 6-substituted pyrrolo[2,3-*d*]pyrimidine to a three-carbon-bridge (analogue **5**) also resulted in an increase of inhibitory activity against the growth of tumor cells in culture compared to the previously reported 6-regioisomer of LY231514.[14] These data suggest that the elongation of the C8−C9 bridge of the classical, 5-substiuted 2,4-diaminofuro[2,3-*d*]pyrimidine and 6-substituted 2-amino-4-oxopyrrolo[2,3-d]pyrimidine are highly conducive to tumor inhibitory activity.

Experimental Section

All evaporations were carried out in vacuo with a rotary evaporator. Analytical samples were dried in vacuo (0.2 mmHg) in a CHEM-DRY drying apparatus over P_2O_5 at 80 °C. Melting points were determined on a MEL-TEMP II melting point apparatus with FLUKE 51 K/J electronic thermometer and are uncorrected. Nuclear magnetic resonance spectra for protons (^{1}H NMR) were recorded on a Bruker WH-300 (300 MHz) spectrometer. The chemical shift values are expressed in ppm (parts per million) relative to tetramethylsilane as internal standard; s = singlet, d = doublet, t = triplet, q = quartet, m = multiplet, br = broad singlet. The relative integrals of peak areas agreed with those expected for the assigned structures. Thin-layer chromatography (TLC) was performed on POLYGRAM Sil G/UV254 silica gel plates with fluorescent indicator, and the spots were visualized under 254 and 366 nm illumination. Proportions of solvents used for TLC are by volume. Column chromatography was performed on 230−400 mesh silica gel purchased from Aldrich, Milwaukee, WI. Elemental analyses were performed by Atlantic Microlab, Inc. Norcross, GA. Element compositions are within ±0.4% of the calculated values. Fractional moles of water or organic solvents frequently found in some analytical samples of antifolates could not be prevented, despite 24−48 h of drying in vacuo, and were confirmed where possible by their presence in the ^{1}H NMR spectra. All solvents and chemicals were purchased from Aldrich Chemical Co. or Fisher Scientific and were used as received.

Methyl 4-(4-Hydroxybutynyl)benzoate (16). To a 250-mL round-bottomed flask, equipped with a magnetic stirrer and gas inlet, was added a mixture of palladium chloride (45 mg, 0.26 mmol), triphenylphosphine (125 mg, 0.48 mmol), methyl 4-bromobenzoate (**14**) (10 g, 46 mmol), and diethylamine (300 mL). To the stirred mixture, under N_2, were added copper(I) iodide (90 mg) and 3-butyn-1-ol (**15**) (3.3 g, 47 mmol), and the reaction mixture was stirred at room temperature overnight (17−18 h). Diethylamine was removed under reduced pressure, brine (80 mL) was added, and the mixture was extracted with EtOAc. The extracts were pooled and dried over Na_2SO_4 and passed over a short silica gel column (3 × 6 cm) to remove the catalyst. The fractions collected were pooled and concentrated under reduced pressure, and the residue was recrystallized from EtOAc/hexane (1:5) to give 8 g (80%) of **16** as white flakes: mp 95.3−96.3 °C (lit. mp 95.5−96 °C); ^{1}H NMR (DMSO-d_6) δ 2.56−2.60 (t, 2 H, propargyl CH_2), 3.56−3.60 (t, 2 H, CH_2−OH), 3.84 (s, 3 H, OMe), 4.92−4.95 (t, 1 H, OH), 7.50−7.53 (d, 2 H, C_6H_4), 7.89−7.92 (d, 2 H, C_6H_4).

Methyl 4-(4-Hydroxybutyl)benzoate (17). To a Parr flask were added **16** (5 g, 25 mmol), 5% palladium on activated carbon (500 mg), and MeOH (100 mL). Hydrogenation was carried out at 45−50 psi of H_2 for 12 h. The reaction mixture was filtered through Celite, washed with MeOH/$CHCl_3$ (1:1) (100 mL), passed through a short silica gel column (3 × 5 cm), and concentrated under reduced pressure to give 5.1 g (quantitative) of **17** as a clear oil: ^{1}H NMR (DMSO-d_6) δ 1.42−1.65 (m, 4 H, 2′-CH_2, 3′-CH_2), 2.60−2.65 (t, 2 H, benzylic CH_2), 3.38−3.42 (t, CH_2−OH), 3.81 (s, 3 H, OMe), 4.39 (br, 1 H, OH), 7.30−7.33 (d, 2 H, C_6H_4), 7.85−7.88 (d, 2 H, C_6H_4). This alcohol was directly used for the next step.

4-(4′-Carbomethoxyphenyl)butyric Acid (18). A solution of methyl 4-(4-hydroxybutyl)benzoate (**17**) (3 g, 15 mmol) in acetone (30 mL) was added dropwise to a cold solution (ice bath) of CrO_3 (8 g) in sulfuric acid (60 mL) and water (180 mL). After the addition, the resulting solution was stirred in an ice bath for an additional 2 h and the solution was allowed to warm to room temperature overnight. TLC indicated the disappearance of the starting alcohol and the formation of one major spot at R_f = 0.35 (hexane/EtOAc 2:1). The solution was

Table 5. Cytotoxicity Evaluation (GI_{50}, M) of Compounds 4 and 5 against Selected NCI Tumor Cell Lines[26]

cell lines	compd **4**	compd **5**	cell lines	compd **4**	compd **5**
leukemia			CNS cancer		
CCRF-CEM	4.29×10^{-8}	4.76×10^{-6}	SF-268	6.48×10^{-7}	5.58×10^{-6}
HL-60(TB)	$<1.0 \times 10^{-8}$	1.11×10^{-6}	melanoma		
K-562	$<1.0 \times 10^{-8}$	6.5×10^{-8}	SK-MEL-28	$>1.0 \times 10^{-4}$	2.95×10^{-7}
SR	$<1.0 \times 10^{-8}$	2.27×10^{-7}	renal cancer		
non-small cell lung cancer			786-0	1.23×10^{-7}	6.28×10^{-7}
A549/ATCC	1.66×10^{-8}	1.70×10^{-7}	prostate cancer		
NCI-H460	$<1.0 \times 10^{-8}$	9.99×10^{-7}	PC-3	1.25×10^{-8}	3.80×10^{-5}
HOP-92	9.59×10^{-5}	4.71×10^{-7}	breast cancer		
colon cancer			MCF7	1.74×10^{-7}	2.21×10^{-6}
HCT-116	$<1.0 \times 10^{-8}$	nd	MDA-MB-435	2.14×10^{-8}	1.30×10^{-6}
SW-620	$<1.0 \times 10^{-8}$	9.56×10^{-7}	MDA-N	2.23×10^{-8}	1.95×10^{-6}

extracted with 3 × 200 mL of ethyl ether and dried over Na_2SO_4. After evaporation of the solvent under reduced pressure, the resulting residue was flash chromatographed through silica gel column (3.5 × 15 cm) using hexane/EtOAc (2:1) as eluent. The desired fraction (TLC) was collected and the solvent evaporated under reduced pressure. Recrystallization of the resulting residue from Et_2O afforded 2 g (63%) of **18** as white crystals: mp 76.5−78 °C; ^{1}H NMR (DMSO-d_6) δ 1.76−1.86 (m, 2 H, β-CH_2), 2.20−2.25 (t, 2 H, α-CH_2), 2.64−2.69 (t, 2 H, benzylic CH_2), 3.83 (s, 3 H, OMe), 7.32−7.35 (d, 2 H, C_6H_4), 7.86−7.89 (d, 2 H, C_6H_4), 12.29 (s, 1 H, COOH). Anal. $C_{12}H_{14}O_4$ (C, H).

Chloromethyl 3-(4′-Carbomethoxyphenyl)propyl Ketone (8). To 4-(4′-carbomethoxyphenyl)butyric acid (**18**) (2.3 g, 10 mmol) in a 100 mL flask were added oxalyl chloride (5 mL) and anhydrous CH_2Cl_2 (10 mL). The resulting solution was refluxed for 1 h and then cooled to room temperature. After evaporating the solvent under reduced pressure, the residue (**19**) was dissolved in 20 mL of Et_2O. The resulting solution was added dropwise to an ice-cooled diazomethane (generated in situ from 15 g of *N*-nitroso-*N*-methylurea) and ether solution in an ice bath over 10 min. The resulting mixture was allowed to stand for 30 min and then stirred for an additional 30 min. To this solution was added concentrated HCl (20 mL). The resulting mixture was refluxed for 1.5 h. After cooling to room temperature, the organic layer was separated and the aqueous layer extracted with Et_2O (100 mL × 2). The combined organic layer and Et_2O extract was washed with two portions of 10% Na_2CO_3 solution and dried over Na_2SO_4. Evaporation of the solvent afforded 2 g (80%) of **8** as yellow needles: mp 30−33 °C; ^{1}H NMR (DMSO-d_6) δ 1.77−1.91 (m, 2 H, β-CH_2), 2.50−2.54 (t, 2 H, α-CH_2), 2.61−2.66 (t, 2 H, benzylic CH_2), 3.82 (s, 3 H, OMe), 4.50 (s, 2 H, CH_2Cl), 7.40−7.43 (d, 2 H, C_6H_4), 7.86−7.89 (d, 2 H, C_6H_4). Anal. $C_{13}H_{15}O_3Cl$ (C, H, Cl).

Methyl 4-[3-(2,4-Diaminofuro[2,3-*d*]pyrimidin-5-yl)-propyl]benzoate (9) and Methyl 4-[3-(2-Amino-3,4-dihydro-4-oxo-7*H*-pyrrolo[2,3-*d*]pyrimidin-6-yl)propyl]benzoate (10). To a suspension of 2,6-diaminopyrimidin-4-one (**7**) (0.8 g, 6 mmol) in anhydrous DMF (15 mL) was added chloromethyl 3-(4′-carbomethoxyphenyl)propyl ketone (**8**) (1.5 g, 6 mmol). The resulting mixture was stirred under N_2 at 40−50 °C for 3 days. TLC showed the disappearance of the starting materials and the formation of two major spots at R_f = 0.58 and 0.39 ($CHCl_3$:MeOH 5:1). After evaporation of solvent under reduced pressure, MeOH (20 mL) was added followed by silica gel (5 g) and the solvent evaporated. The resulting plug was loaded on to a silica gel column (3.5 × 12 cm) and eluted with $CHCl_3$ followed by 3% MeOH in $CHCl_3$ and then 4% MeOH in $CHCl_3$. Fractions with an R_f = 0.58 (TLC) were pooled and evaporated and the resulting residue was recrystallized from MeOH to afford 800 mg (40%) of **9** as white crystals: mp 221.2−222.8 °C; ^{1}H NMR (DMSO-d_6) δ 1.80−1.88 (m, 2 H, C9−CH_2), 2.57−2.65 (t, 2 H, C10−CH_2), 2.69−2.75 (t, 2 H, C8−CH_2), 3.82 (s, 3 H, OMe), 5.96 (s, 2 H, 2-NH_2), 6.47 (s, 2 H, 4-NH_2), 7.13 (s, 1 H, C6−CH), 7.35−7.37 (d, 2 H, C_6H_4), 7.86−7.88 (d, 2 H, C_6H_4). Anal. $C_{17}H_{18}N_4O_3$ (C, H, N).

Fractions with R_f = 0.38 (TLC) were pooled and evaporated, and the resulting residue was recrystallized from CH_3OH (10 mL) to afford 800 mg (40%) of **10** as light yellow crystals: mp 240.2−242 °C; ^{1}H NMR (DMSO-d_6) δ 1.83−1.95 (m, 2 H, C9−CH_2), 2.64−2.69 (t, 2 H, C10−CH_2), 2.73−2.97 (two sets of t, 2 H, C8−CH_2), 3.82 (s, 3 H, OMe), 5.89 (s, 1 H, C5−CH), 5.96 (s, 2 H, 4-NH_2), 7.34−7.37 (d, 2 H, Ph-CH), 7.86−7.89 (d, 2 H, Ph-CH), 10.15 (s, 1 H, 3-NH), 10.83 (s, 1 H, 7-NH). Anal. $C_{17}H_{18}N_4O_3 \cdot 0.2H_2O$ (C, H, N).

4-[3-(2,4-Diaminofuro[2,3-*d*]pyrimidin-5-yl)propyl]-benzoic Acid (20). To a suspension of the ester **9** (300 mg, 9 mmol) in MeOH/DMSO (1:1) (40 mL) was added 3 N NaOH (15 mL). The resulting mixture was stirred at 40−50 °C under N_2 for 5 h. TLC indicated the disappearance of starting material and the formation of one major spot at the origin. The resulting solution was passed through Celite and washed with a minimum amount of CH_3OH. The combined filtrate was evaporated under reduced pressure to dryness. To this residue was added distilled water (15 mL), the resulting solution was cooled in an ice bath, and the pH was adjusted to 3 to 4 using 3 N HCl. The resulting suspension was frozen using a dry ice−acetone bath and thawed to 4 °C overnight in a refrigerator. The suspension was filtered, washed with cold water, and dried in a desiccator using P_2O_5 under reduced pressure to afford 280 mg (92%) of **20** as a white powder: mp >370 °C (dec); R_f = 0.38 ($CHCl_3$/MeOH 5:1); ^{1}H NMR (DMSO-d_6) δ 1.80−1.85 (m, 2 H, C9−CH_2), 2.65−2.95 (m, 4 H, C10−CH_2, C8−CH_2), 6.85 (s, 2 H, 2- or 4-NH_2), 7.20−7.39 (m, 5 H, 4- or 2-NH_2, C6−CH, C_6H_4), 7.84−7.86 (d, 2 H, C_6H_4), 12.80 (s, 1 H, COOH). Anal. $C_{16}H_{16}N_4O_3 \cdot 1.0HCl \cdot 0.30H_2O$ (C, H, N). This acid was used directly for the next step without further purification.

Diethyl *N*-{4-[3-(2,4-Diaminofuro[2,3-*d*]pyrimidin-5-yl)propyl]benzoyl}-L-glutamate (22). To a solution of **20** (200 mg, 0.57 mmol) in anhydrous DMF (9 mL) was added triethylamine (200 μL) and the mixture stirred under N_2 at room temperature for 5 min. The resulting solution was cooled to 0° C, isobutyl chloroformate (200 μL, 1.5 mmol) was added, and the mixture was stirred at 0° C for 30 min. At this time TLC (MeOH/$CHCl_3$ 1:5) indicated the formation of the activated intermediate (R_f = 0.62) and the disappearance of the starting acid (R_f = 0.38). Diethyl-L-glutamate hydrochloride (390 mg, 1.5 mmol) was added to the reaction mixture followed immediately by triethylamine (200 μL, 1.5 mmol). The reaction mixture was slowly allowed to warm to room temperature and stirred under N_2 for 18 h. The reaction mixture was then subjected to another cycle of activation and coupling using half the quantities listed above. The reaction mixture was slowly allowed to warm to room temperature and stirred under N_2 for an additional 24 h. TLC showed the formation of one major spot at R_f = 0.62 (MeOH/$CHCl_3$ 1:5). The reaction mixture was evaporated to dryness under reduced pressure. The residue was dissolved in a minimum amount of MeOH/CH_3Cl (1:4) and chromatographed on a silica gel column (2 × 15 cm) with 2% MeOH in $CHCl_3$ as eluent. The desired fractions (TLC) were pooled and evaporated to dryness, and the residue was crystallized from Et_2O to afford 240 mg (60%) of **22** as yellow needles: mp 130.6−132.2 °C; ^{1}H NMR (DMSO-d_6) 1.08−1.25 (m, 6 H, OEt), δ 1.78−1.80 (m, 2 H, C9−CH_2), 1.97−2.11 (2

sets of t, 2 H, Glu β-CH_2), 2.40−2.45 (t, 2 H, Glu γ-CH_2), 2.57−2.80 (m, 4 H, C10−CH_2, C8−CH_2), 4.00−4.13 (m, 4 H, OEt), 4.33−4.40 (m, 1 H, Glu α-CH), 5.97 (s, 2 H, 4-NH_2), 6.41 (s, 2 H, 2-NH_2), 7.13 (s, 1 H, C6−CH), 7.33−7.35 (d, 2 H, C_6H_4), 7.79−7.81 (d, 2 H, C_6H_4), 8.64−8.66 (d, 1 H, −CONH−). Anal. $C_{25}H_{31}N_5O_6$ (C, H, N).

***N*-{4-[3-(2,4-Diaminofuro[2,3-*d*]pyrimidin-5-yl)propyl]-benzoyl}-L-glutamic Acid (4).** To a solution of the diester **22** (150 mg, 0.3 mmol) in MeOH (10 mL) was added 1 N NaOH (6 mL) and the mixture was stirred under N_2 at room temperature for 16 h. TLC showed the disappearance of the starting material (R_f = 0.62) (MeOH/$CHCl_3$ 1:5) and formation of one major spot at the origin. The reaction mixture was evaporated to dryness under reduced pressure and the residue dissolved in water (10 mL). The resulting solution was cooled in an ice bath and the pH adjusted to 3−4 with dropwise addition of 1 N HCl. The resulting suspension was frozen in a dry ice−acetone bath, thawed in the refrigerator to 4−5 °C, and filtered. The residue was washed with a small amount of cold water and ethyl acetate and dried in vacuo using P_2O_5 to afford 130 mg (92%) of **4** as a white powder: mp 159−161 °C; ^{1}H NMR (DMSO-d_6) 1.83−2.08 (m, 4 H, C9−CH_2, Glu β-CH_2), 2.32−2.36 (t, 2 H, Glu γ-CH_2), 2.57−2.93 (m, 4 H, C10−CH_2, C8−CH_2), 4.36−4.38 (m, 1 H, Glu α-CH), 5.97 (s, 2 H, 4-NH_2), 6.40 (s, 2 H, 2-NH_2), 7.13 (s, 1 H, C6−CH), 7.30−7.32 (d, 2 H, C_6H_4), 7.80−7.82 (d, 2 H, C_6H_4), 8.50−8.52 (d, 1 H, −CONH−), 12.38−12.53 (br, 2 H, 2 × COOH). Anal. $C_{21}H_{23}N_5O_6$·1.2H_2O (C, H, N).

4-[3-(2-Amino-3,4-dihydro-4-oxo-7*H*-pyrrolo[2,3-*d*]-pyrimidin-6-yl)propyl]benzoic Acid (21). To a suspension of **10** (250 mg, 7 mmol) in CH_3OH/DMSO (1:1) was added 15 mL of 3 N NaOH. The resulting mixture was stirred under N_2 at 40−50 °C for 5 h. TLC indicated the disappearance of starting material and the formation of one major spot at the origin. The resulting solution was passed through Celite and washed with a minimum amount of CH_3OH. The combined filtrate was evaporated under reduced pressure to dryness. To this residue was added 15 mL of distilled water, and the solution, in an ice bath, was adjusted to pH 3−4 using 2 N HCl. The resulting suspension was frozen in an acetone−dry ice bath, thawed to 4 °C overnight in a refrigerator, filtered, washed with cold water, and dried in a desiccator under reduced pressure using P_2O_5 to afford 260 mg (90%) of **21**: mp >280 °C (dec); R_f = 0.32 ($CHCl_3$: MeOH 5:1); ^{1}H NMR (DMSO-d_6) δ 1.88−1.97 (m, 2 H, C9−CH_2), 2.66−2.97 (m, 4 H, C10−CH_2, C8−CH_2), 5.96 (s, 1 H, C5−CH), 6.60 (br, 2 H, 2-NH_2), 7.32−7.34 (d, 2 H, C_6H_4), 7.85−7.87 (d, 2 H, C_6H_4), 10.68 (s, 1 H, 3-NH), 11.17 (s, 1 H, 7-NH), 13.0 (s, 1 H, COOH). Anal. $C_{16}H_{16}$ N_4O_3·1.0HCl·0.30H_2O (C, H, N). This acid was used directly for the next step without further purification.

***N*-{4-[3-(2-Amino-3,4-dihydro-4-oxo-7*H*-pyrrolo[2,3-*d*]-pyrimidin-6-yl)propyl]benzoyl}-L-glutamic Acid (5).** To a solution of **21** (200 mg, 0.57 mmol) in anhydrous DMF (9 mL) was added triethylamine (200 μL) and the mixture stirred under N_2 at room temperature for 5 min. The resulting solution was cooled to 0 °C, isobutyl chloroformate (200 μL 1.5 mmol) was added, and the mixture was stirred at 0 °C for 30 min. At this time, TLC (MeOH/$CHCl_3$ 1:5) indicated the formation of the activated intermediate at R_f 0.44 and the disappearance of the starting acid (R_f 0.32). Diethyl-L-glutamate hydrochloride (390 mg, 1.5 mmol) was added to the reaction mixture followed immediately by triethylamine (200 μL, 1.5 mmol). The reaction mixture was slowly allowed to warm to room temperature and stirred under N_2 for 18 h. The reaction mixture was then subjected to another cycle of activation and coupling using half the quantities listed above. The reaction mixture was slowly allowed to warm to room temperature and stirred under N_2 for 24 h. TLC showed the formation of one major spot at R_f = 0.45 (MeOH/$CHCl_3$ 1:5). The reaction mixture was evaporated to dryness under reduced pressure. The residue was dissolved in a minimum amount of CH_3Cl/MeOH (4:1) and chromatographed on a silica gel column (2 × 15 cm) with 4% MeOH in $CHCl_3$ as the eluent. Fractions that showed the desired single spot at R_f = 0.45 were pooled and evaporated to dryness to afford 240 mg (60%) of **23** as a yellow syrup which was used directly for the next step.

To a solution of the diester **23** (150 mg, 0.3 mmol) in MeOH (10 mL) was added 1 N NaOH (6 mL) and the mixture was stirred under N_2 at room temperature for 16 h. TLC showed the disappearance of the starting material (R_f = 0.45) and one major spot at the origin (MeOH/$CHCl_3$ 1:5). The reaction mixture was evaporated to dryness under reduced pressure. The residue was dissolved in water (10 mL), the resulting solution was cooled in an ice bath, and the pH was adjusted to 3−4 with dropwise addition of 1 N HCl. The resulting suspension was frozen in a dry ice−acetone bath, thawed to 4−5 °C in the refrigerator, and filtered. The residue was washed with a small amount of cold water and ethyl acetate and dried in vacuo using P_2O_5 to afford 135 mg (95%) of **5** as a yellow powder: mp 187.1−190 °C; ^{1}H NMR (DMSO-d_6) δ 1.87−2.11 (m, 4 H, C9−CH_2, Glu β-CH_2), 2.33−2.38 (t, 2 H, Glu γ-CH_2), 2.47−2.68 (m, 4 H, C10−CH_2, C8−CH_2), 4.38−4.43 (m, 1 H, Glu α-CH), 5.89 (s, 1 H, C5−CH), 6.02 (s, 2 H, 2-NH_2), 7.30−7.32 (d, 2 H, C_6H_4), 7.78−7.80 (d, 2 H, C_6H_4), 8.52−8.54 (d, 1 H, −CONH), 10.19 (s, 1 H, 3-NH), 10.82 (s, 1 H, 7-NH). Anal. ($C_{21}H_{23}N_5O_6$·1.0HCl) (C, H, N, Cl)

Dihydrofolate Reductase (DHFR) Assay.[29] All enzymes were assayed spetrophotometrically in a solution containing 50 μM dihydrofolate, 80 μM NADPH, 0.05 M Tris-HCl, 0.001 M 2-mercaptoethanol, and 0.001 M EDTA at pH 7.4 and 30 °C. The reaction was initiated with an amount of enzyme yielding a change in OD at 340 nm of 0.015/min.

Thymidylate Synthase (TS) Assay. TS was assayed spectrophotometrically at 30 °C and pH 7.4 in a mixture containing 0.1 M 2-mercaptoethanol, 0.0003 M (6*R*,*S*)-tetrahydrofolate, 0.012 M formaldehyde, 0.02 M $MgCl_2$, 0.001 M dUMP, 0.04 M Tris-HCl, and 0.00075 M NaEDTA. This was the assay described by Wahba and Friedkin,[30] except that the dUMP concentration was increased 25-fold according to the method of Davisson et al.[31] The reaction was initiated by the addition of an amount of enzyme yielding a change in absorbance at 340 nm of 0.016/min in the absence of inhibitor.

Cell Lines and Methods for Measuring Growth Inhibitory Potency (Table 2). Drug solutions were standardized using extinction coefficients. Extinction coefficients were determined for **4** [pH 1, λ_{max-1} 249 nm (21 500), λ_{max-2} 302 nm (7100); pH 7, λ_{max} 250 nm (21 100); pH 13, λ_{max} 251 nm (21 300)] and for **5** [pH 1, λ_{max} 229 nm (21 900); pH 7, λ_{max} 251 nm (20 900); pH 13, λ_{max} 251 nm (20 600)]. Extinction coefficients for methotrexate (MTX), a gift of Immunex (Seattle, WA), were from the literature.[32] Aminopterin, hypoxanthine (Hx), thymidine (TdR), and deoxycytidine (dCyd) were purchased from Sigma Chemical Co. (St. Louis, MO). Calcium leucovorin (LV) was purchased from Schircks Laboratories (Jona, Switzerland). Other chemicals and reagents were reagent grade or higher.

Cell lines were verified to be negative for mycoplasma contamination (Mycoplasma Plus PCR primers, Stratagene, La Jolla, CA). The human T-lymphoblastic leukemia cell line CCRF-CEM[21] and its MTX-resistant sublines R1,[22] R2,[23] and R30dm[24] were cultured as described.[24] R1 expresses 20-fold elevated levels of dihydrofolate reductase (DHFR), the target enzyme of MTX. R2 has dramatically reduced MTX uptake but normal levels of MTX-sensitive DHFR. R30dm expresses 1% of the folylpolyglutamate synthetase (FPGS) activity of CCRF-CEM and is resistant to short-term, but not continuous, MTX exposure; however, R30dm is cross-resistant in continuous exposure to antifolates that require polyglutamylation to form potent inhibitors. Growth inhibition of all cell lines by continuous drug exposure was assayed as described.[20,24] EC_{50} values (drug concentration effective at inhibiting cell growth by 50%) were determined visually from plots of percent growth relative to a solvent-treated control culture versus the logarithm of drug concentration.

Protection against growth inhibition of CCRF-CEM cells was assayed by including leucovorin ((6*R*,*S*)-5-formyltetrahydrofolate) at 0.1−10 μM with a concentration of drug previously determined to inhibit growth by 90−95%; the remainder of

the assay was as described. Growth inhibition was measured relative to the appropriate leucovorin-treated control; leucovorin, even at 10 μM, caused no growth inhibition in the absence of drug, however. Protection against growth inhibition of CCRF-CEM cells was assayed by including Hx (10 μM), TdR (5 μM), or dCyd (10 μM) individually, in pairs (Hx + dCyd, TdR + dCyd), or all together (Hx + TdR + dCyd) with concentrations of MTX, **4**, or **5** that would inhibit growth by 90−95% over a growth period of ≈72 h. Compound **4** could only be tested up to 1500 nM, a concentration that inhibited growth by only 80%. The growth period was limited, because beyond 72 h CCRF-CEM cells deplete TdR in the growth media and drug effects are no longer protected. dCyd is added only to alleviate the growth inhibitory effects of 5 μM TdR against CCRF-CEM cells.[33] Controls with metabolites alone (no drug) in the combinations described above (in duplicate), controls with drug alone with no metabolites (in duplicate), and untreated controls with neither drugs nor metabolites (in quadruplicate) were performed. Growth inhibition was measured as percent growth relative to untreated control cells (absence of drugs and metabolites).

Folylpolyglutamate Synthetase (FPGS) Purification and Assay. Recombinant human cytosolic FPGS was purified and assayed as described previously.[11] Both **4** and **5** were themselves quantitatively recovered during the standard assay procedure, thus ensuring that their polyglutamate products would also be quantitatively recovered. Kinetic constants were determined by the hyperbolic curve fitting subroutine of SigmaPlot (Jandel) or Kaleidagraph (Synergy Software) using a ≥10-fold range of substrate concentration. Activity was linear with respect to time at the highest and lowest substrate concentrations tested. Assays contained ≈400 units of FPGS activity; one unit of FPGS catalyzes incorporation of 1 pmol of [^{3}H]glutamate/h. Because K_m values for **4** and **5** were low, the assays to determine kinetic constants were modified to include 2 mM L-[^{3}H]glutamate, instead of the standard 4 mM. The resulting lower background allowed quantitation at lower levels of product synthesis. The K_m value for AMT was the same whether 2 or 4 mM glutamate was used (data not shown).

Acknowledgment. This work was supported in part by grants from the National Institute of Health CA89300 (A.G.), AI44661 (A.G.), CA43500 (J.J.M.) and Roswell Park Cancer Institute Core Grant CA16065 from the NCI, and CA10914 (R.L.K.). The authors thank Mr. William Haile for performing growth inhibition studies and FPGS activity assays.

Supporting Information Available: Elemental analysis data for **4**, **5**, **8**−**10**, **18**, **20**−**22**. This material is available free of charge via the Internet at http://pubs.acs.org.

References

(1) Presented, in part, at the 221st American Chemical Society National Meeting, San Diego, CA, April 2001; MEDI 133.
(2) Berman, E. M.; Werbel, L. M. The Renewed Potential for Folate Antagonists in Contemporary Cancer Chemotherapy. *J. Med. Chem.* **1991**, *34*, 479−485.
(3) Rosowsky, A. Chemistry and Biological Activity of Antifolates. In *Progress in Medicinal Chemistry*; Ellis, G. P., West, G. B., Eds.; Elsevier Science Publishers: Amsterdam, 1989; pp 1−252.
(4) Gangjee, A.; Elzein, E.; Kothare, M.; Vasudevan, A. Classical and Nonclassical Antifolates as Potential Antitumor, Antipneumocystis and Antitoxoplasma Agents. *Curr. Pharm. Design* **1996**, *2*, 263−280.
(5) Gangjee, A.; Devraj, R.; McGuire, J. J.; Kisliuk, R. L. Effect of Bridge Region Variation on Antifolate and Antitumor Activity of Classical 5-Substituted 2,4-Diaminofuro[2,3-*d*]pyrimidines. *J. Med. Chem.* **1995**, *38*, 3798−3805.
(6) Gangjee, A.; Zeng, Y.; McGuire, J. J.; Kisliuk, R. L. Effect of C9-Methyl Substitution and C8−C9 Conformational restriction on Antifolate and Antitumor Activity of Classical 5-Substituted 2,4-Diaminofuro[2,3-*d*]pyrimidines. *J. Med. Chem.* **2000**, *43*, 3125−3133.
(7) Gangjee, A.; Zeng, Y.; McGuire, J. J.; Kisliuk, R. L. Synthesis of *N*-[4-[1-Ethyl-2-(2,4-diaminofuro[2,3-*d*]pyrimidin-5-yl)ethyl]-benzoyl]-L-glutamic acid as an Antifolate. *J. Med. Chem.* **2002**, *45*, 1942−1948.
(8) Tripos Inc., 1699 South Handley Rd, Suite 303, St. Louis, MO 63144.
(9) Cody, V.; Wojtczak, A.; Kalman, T. I.; Friesheim, J. H.; Blakley, R. L. Conformational Analysis of Human Dihydrofolate Reductase Inhibitor Complexes: Crystal Structure Determination of Wild-Type and F31 Mutant Binary and Ternary Inhibitor Complexes. In *Advances in Experimental Medicine and Biology, Chemistry, and Biology of Pteridines and Folates;* Ayling, J. E., Nair, M. G., Baugh, C. M., Eds.; Plenum Press: New York, 1993; Vol. 338, pp 481−486.
(10) Miwa, T.; Hitaka, T.; Akimoto, H.; Nomura, H. Novel Pyrrolo-[2,3-*d*]pyrimidine Antifolates: Synthesis and Antitumor Activities. *J. Med. Chem.* **1991**, *34,* 555−560.
(11) Gangjee, A.; Yu, J.; McGuire, J. J.; Cody, V.; Galitsky, N.; Kisliuk, R. L.; Queener, S. F. Design, Synthesis, and X-ray Crystal Structure of a Potent Dual Inhibitor of Thymidylate Synthase and Dihydrofolate Reductase as an Antitumor Agent. *J. Med. Chem.* **2000**, *43*, 3837−3851.
(12) Taylor, E. C.; Kuhnt, D.; Shih, C.; Rinzel, S. M.; Grindey, G. B.; Barredo, J.; Lannatipour, M.; Moran, R. A Dideazatetrahydrofolate Analogue Lacking a Chiral Center at C6, *N*-[4-[2-(2-Amino-3,4-dihydro-4-oxo-7*H*-pyrrolo[2,3-*d*]pyrimidine-5-yl)ethyl]-benzoyl]-L-glutamic Acid, Is an Inhibitor of Thymidylate Synthase. *J. Med. Chem.* **1992**, *35*, 4450−4454.
(13) Anderson, A. C.; Perry, K. M.; Freymann, D. M. and Stroud, R. M. The Crystal Structure of Thymidylate Synthase From *Pneumocystis carinii* Reveals a Fungal Insert Important for Drug Design. *J. Mol. Biol.* **2000**, *297*, 645−657.
(14) Shih, C.; Barnett, C. J.; Grindey, G. B.; Pearce, H. L.; Engelhardt, J. A.; Todd, G. C.; Rinzel, S. M.; Worzalla, J. F.; Gossett, L. S.; Everson, T. P.; Wilson, T. M.; Kobierski, M. E.; Winter, M. A.; Moran, R. G.; Kuhnt, D.; Taylor, E. C. Structural Features That Determine the Biological Activity of Pyrrolo[2,3-*d*]pyrimidine Based Antifolates. Presented at the Tenth International Symposium, Chemistry and Biology of Pteridines and Folates, Orange Beach, AL, March 21−26, 1993; Abstr F 15.
(15) Secrist, J. A., III; Liu, P. S. Studies Directed Toward a Total Synthesis of Nucleoside Q. The Annulation of 2,4-Diaminopyrimidin-4-one with (α-Halo Carbonyls To Form Pyrrolo[2,3-*d*]pyrimidines and Furo[2,3-*d*]pyrimidines. *J. Org. Chem.* **1978***, 43,* 3937−3941.
(16) Gangjee, A.; Yang, J.; McGuire, J. J.; Kisliuk, R. L. Classical 2,4-Diamino-5-substituted Furo[2,3-*d*]pyrimidine and 2-Amino-4-oxo-6-substituted Pyrrolo[2,3-*d*]pyrimidine on Antifolate Activity. In *Chemistry and Biochemistry of Pteridines and Folates;* Milstien, S., Kapatos, G., Levine, R. A., Shane, B., Eds.; Kluwer Academic Publishers: Boston, 2002; pp 445−450.
(17) Taylor, E. C.; Harrington, P. M. A Convergent Synthesis of 5, 10-Dideaza-5,6,7,8-tetrahydrofolic Acid and 5,10-Dideaza-5,6,7,8-tetrahydrohomofolic Acid. An Effective Principle for Carbonyl Group Activation. *J. Org. Chem.* **1990**, *55*, 3222−3227.
(18) Wipf, P.; Coish, P. D. G. Total Synthesis of (±)-Nisamycin. *J. Org. Chem.* **1999**, *64*, 5053−5061.
(19) DeGraw, J. L.; Kisliuk, R. L.; Gaumont, Y.; Baugh, C. M.; Nair, M. G. Synthesis and Antifolate Activity of 10-Deazaaminopterin. *J. Med. Chem.* **1974***, 17,* 552−553.
(20) McGuire, J. J.; Magee, K. J.; Russell, C. A.; Canestrari, J. M. Thymidylate Synthase as a Target for Growth Inhibition in Methotrexate-Sensitive and -Resistant Human Head and Neck Cancer and Leukemia Cell Lines. *Oncology Res.* **1997**, *9,* 139−147.
(21) Foley, G. F.; Lazarus, H.; Farber, S.; Uzman, B. G.; Boone, B. A.; McCarthy, R. E. Continuous Culture of Lymphoblasts from Peripheral Blood of a Child with Acute Leukemia. *Cancer* **1965**, *18*, 522−529.
(22) Mini, E.; Srimatkandada, S.; Medina, W. D.; Moroson, B. A.; Carman, M. D.; Bertino, J. R. Molecular and Karyological Analysis of Methotrexate-Resistant and -Sensitive Human Leukemic CCRF-CEM Cells. *Cancer Res.* **1985**, *45*, 317−325.
(23) Rosowsky, A.; Lazarus, H.; Yuan, G. C.; Beltz, W. R.; Mangini, L.; Abelson, H. T.; Modest, E. J.; Frei, E., III. Effects of Methotrexate Esters and Other Lipophilic Antifolates on Methotrexate-Resistant Human Leukemic Lymphoblasts. *Biochem. Pharmacol.* **1980**, *29*, 648−652.
(24) McCloskey, D. E.; McGuire, J. J.; Russell, C. A.; Rowan, B. G.; Bertino, J. R.; Pizzorno, G.; Mini, E. Decreased Folylpolyglutamate Synthetase Activity as a Mechanism of Methotrexate Resistance in CCRF-CEM Human Leukemia Sublines. *J. Biol. Chem.* **1991**, *266*, 6181−6187.

(25) Wong, S. C.; Zhang, L.; Witt, T. L.; Proefke, S. A.; Bhushan, A.; Matherly, L. H. Impaired Membrane Transport in Methotrexate-Resistant CCRF-CEM Cells Involves Early Translation Termination and Increased Turnover of a Mutant Reduced Folate Carrier. *J. Biol. Chem.* **1999**, *274*, 10388−10394.
(26) Hakala, M. T.; Taylor, E. The Ability of Purine and Thymidine Derivatives and of Glycine To Support the Growth of Mammalian Cells in Culture. *J. Biol. Chem.* **1959**, *234*, 126−128.
(27) McGuire, J. J. Anticancer Antifolates: Current Status and Future Directions. *Curr. Pharm. Design* **2003**, *9*, 2593−2613.
(28) We thank the Developmental Therapeutics Program of the National Cancer Institute for performing the in vitro anticancer evaluation.
(29) Kisliuk, R. L.; Strumpf, D.; Gaumont, Y.; Leary, R. P.; Plante, L. Diastereoisomers of 5,10-Methylene-5,6,7,8-tetrahydropteroyl-D-glutamic Acid. *J. Med. Chem.* **1977**, *20*, 1531−1533.
(30) Wahba, A. J.; Friedkin, M. The Enzymatic Synthesis of Thymidylate. Early Step in the Purification of Thymidylate Synthetase of *Escherichia coli*. *J. Biol. Chem*. **1962**, *237*, 3794−3801.
(31) Davissson, V. J.; Sirawaraporn, W.; Santi, D. V. Expression of Human Thymidylate Synthase in *Escherichia coli*. *J. Biol. Chem*. **1989**, *264*, 9145−9148.
(32) Blakley, R. L. *The Biochemistry of Folic Acid and Related Pteridines;* Elsevier: Amsterdam, 1969, p 569.
(33) Grindey, G. B.; Wang, M. C.; Kinahan, J. J. Thymidine Induced Perturbations in Ribonucleoside and Deoxyribonucleoside Triphosphate Pools in Human Leukemic CCRF-CEM Cells. *Mol. Pharmacol.* **1979**, *16*, 601−606.

JM040123K